Cyclic fatigue failure of TPU using a crack propagation approach

Giorgia Scetta [a], Nathan Selles [b], Patrick Heuillet [b], Matteo Ciccotti [a,*], Costantino Creton [a,**]

[a] Sciences et Ingénierie de La Matière Molle, ESPCI Paris, Université PSL, CNRS, Sorbonne Université, 75005, Paris, France
[b] Laboratoire de Recherches et de Contrôle Du Caoutchouc et des Plastiques, 60, Rue Auber, 94408, Vitry-sur-Seine, France

A B S T R A C T

Thermoplastic polyurethane elastomers (TPU) are stretchable, tough, wear resistant and easily processable soft materials. Especially because of their recyclability, TPUs can be suitable candidates to replace rubbers in several applications such as damping, footwear and cable coatings. However, their capacity to operate under cyclic loads over many cycles was rarely investigated, mainly due to their complex strain-dependent morphology and vis-coplastic character. Additionally, the absence of chemical crosslinks results in a certain degree of creep and plastic deformation when TPUs are cyclically strained, questioning how to unambiguously define fracture mechanics variables such as the energy release rate G, typically used to evaluate fatigue crack growth in chemically crosslinked elastomers. We show that, when TPUs are cyclically loaded up to the same value of maximum stretch, their stress-stretch curve changes with the number of applied cycles, but eventually achieves a steady-state. We propose a suitable methodology to evaluate the cyclic fatigue resistance in TPUs, based on a fracture mechanics approach with some additional treatments to account for the higher tendency to creep of TPUs than thermoset rubbers. Comparing the obtained results of TPU with those for classical filled rubbers with a similar small strain modulus, we underline the excellent toughness and cyclic fatigue resistance of TPUs, opening new opportunities in their use for applications requiring to resist to crack propagation under cyclic loading at large strains.

1. Introduction

Thermoplastic polyurethanes elastomers (TPU) are an interesting class of thermoplastic materials that appeared on the market around 1960 [1]. Soft TPUs display a rubberlike behaviour at ambient temperature without any need for chemical crosslinking. They are typically composed of long polyether or aliphatic polyester flexible chains called soft segment (SS) and short sequences containing an isocyanate linked with a short chain extender called hard segments (HS). Because of their chemical incompatibility SS and HS tend to separate in a two-phase system, while the presence of inter-hydrogen bonding between ure-thane units causes the HS to aggregate in small and hard domains (HD) of nanometric dimensions. These HS clusters connect the polymer chains with physical links, as schematically showed in Fig. 1 (a), and prevents them to flow at working temperature. When the softening temperature of the hard phase is reached, the polymer flows and can be easily and reversibly shaped. The properties of TPU can be tuned to achieve specific strength and elasticity by changing the chemical nature and relative proportion of either the hard-polyurethane group or the long soft

segment. The HS microdomains are generally sufficient to reinforce the materials without any additional filler. Classical elastomers on the other hand (Fig. 1 (b)), need to be chemically crosslinked and filled (with carbon black and/or silica) to show the combination of reversible elasticity and toughness typical of commercial rubber.

The peculiar microstructure of TPU provides them with some advantages compared with conventional rubbers such as the possibility to be easily processed and reprocessed through rapid processing techniques as injection moulding and extrusion. Moreover, they also possess an excellent abrasion resistance as well as blood and tissue compatibility, so that they have been rapidly used in numerous applications such as footwear, medical cables, wheels or dampers. Nevertheless, the suitability of TPUs in applications requiring the material to sustain cyclical loads and to prevent sudden failure or fatigue crack growth requires a robust characterization method in cyclic fatigue. Opposite to rubbers, where cyclic fatigue resistance has been thoroughly studied [2, 3], only few investigations have been carried out in TPUs [4–6]. This shortcoming mainly comes from the complex visco-plastic character of TPUs at large strains. The mechanical properties of TPUs are indeed

---

* Corresponding author.
** Corresponding author.
E-mail addresses: matteo.ciccotti@espci.psl.eu (M. Ciccotti), Costantino.creton@espci.psl.eu (C. Creton).

deeply related to their complex strain-dependent morphology [7–10]. The change in size and orientation of HD with the application of strain, induces mechanical hysteresis in cyclic loading and a permanent modification of the small-strain modulus and maximum extensibility of the material. Additionally, the absence of chemical crosslinking generates a significant residual plastic strain (and stress softening) that increases with cyclic sample deformation. Such complex change in structure and strain dependent properties are not straightforward to include in the common framework of fracture mechanics used to assess cyclic fatigue in rubbers that are instead mostly elastic. In this work, we use a pure shear geometry (PS) to investigate how a crack propagates in a typical commercial soft TPU submitted to a cyclic loading. We used two different testing protocols and assessed their suitability and the effect on the crack propagation rate. Finally, within the context of possible replacement of filled rubbers with soft TPU and in order to highlight the key differences between these classes of materials, we compared our fatigue results on TPU with those obtained on a filled SBR having a similar shore hardness and small-strain modulus which in principle could be used in similar industrial applications.

1.1. The classic fracture mechanics approach for cyclic fatigue in rubbers and calculation of G

Since the last century, the field of cyclic fatigue resistance was largely developed for crosslinked elastomers [3,11] and two main approaches have been used to define their cyclic fatigue resistance: onset of crack nucleation [12,13] and crack propagation rate [14,15]. The first method defines fatigue resistance as the maximum number of cycles at a given strain or stress to achieve a definite loss in strength or end of life of the material. The second one seeks to evaluate the crack growth rate of a pre-existing crack per cycle as a function of applied energy release rate G [16]. We focused on the second approach that has in our view several advantages:

- The use of the energy release rate G (instead of strain or stress) allows to compare samples of different sizes tested under different loading conditions.
- Opposite to crack nucleation, where small defects (that are potentially precursors of the macroscopic failure) are randomly distributed in the sample, in notched samples the macroscopic cut dominates over all the pre-existent defects leading to more reproducible results.
- It is suitable for applications where cracks are nucleated from the start, but lifetime is limited by propagation.

Fatigue resistance is generally expressed in terms of crack propagation per cycle dc/dn vs. maximum applied energy release rate G. As reported in the literature [15,17], irrespectively of their composition elastomers typically show similar trends of dc/dn vs. G, which can be summarized as follows: for values of G lower than a critical threshold G_t and in the absence of any chemical attack, the crack does not propagate. For $G > G_t$, dc/dn can be described by a monotonically growing function of G, which presents a linear region for small G, followed by a power law

for larger G. Finally, for G larger than a critical value G_c, generally named "toughness" in the literature of filled rubbers, a catastrophic propagation is observed and the material ruptures in a few cycles. Following the crack propagation approach, fatigue resistance in rubbers is typically carried out using samples in the pure shear geometry (PS) [18] which corresponds to a wide and thin rectangular shape. One of the main advantages of using the PS geometry is that it allows an easy evaluation of the energy release rate $G(\lambda)$ as a function of the applied stretch λ, which is independent of crack length as shown by the seminal work of Rivlin and Thomas [16] and can be calculated as:

$$G(\lambda) = W(\lambda)h_0 \tag{1}$$

where $W(\lambda)$ is the integral under the stress-strain curve of an unnotched sample with the same geometry.

A common approach to calculate $G(\lambda)$ in filled rubbers is to pre-strain (or precondition) the unnotched sample for some thousands of cycles at higher values of λ than those used in fatigue testing and then to evaluate $G(\lambda)$ by cyclically straining the accommodated sample at different values of increasing stretch. In this way, most of transient effects related to Mullins damage in the first cycles are avoided in the calculation of the relevant G for long term cyclic fatigue.

Applying this method to TPUs without modification creates several challenges that are the focus of this paper. The first issue is that TPUs typically show significant residual deformation when unloaded. While the sample is cyclically loaded at a constant maximum applied stretch, the residual deformation increases during cycles, and hence the stress-stretch curve is modified and the actual energy release rate seen by the crack is not constant. Unlike conventional rubbers, the applied energy release rate G is a function of both the maximum applied stretch and the number of cycles (n): $G(\lambda,n)$. Moreover, if the sample is allowed to unload up to $\lambda_{min} = 1$, calculated using the initial height h_0 of the pristine sample, the residual plastic stretch causes an extensive buckling during unloading cycles that may induce additional undesirable damage in the sample. Furthermore, since TPUs are typically tested in cyclic fatigue at significantly larger stretch than filled rubbers (as will be showed in Section 4.3), a second important issue needs to be addressed. The well-established pre-conditioning procedure cannot be easily implemented to eliminate transient effects, since it would involve very large stretch that are likely to damage the sample. Also, if the sample is preconditioned to a stretch λ_p that is only slightly larger than the cyclic stretch λ to be tested, the values of the energy release rate will depend on this maximum stretch: $G(\lambda,\lambda_p)$ applied during the preconditioning. Defining in which conditions should the cyclic load be applied in TPU to obtain reliable and reproducible crack propagation data is precisely the objective of this work.

2. Materials and methods

2.1. TPU

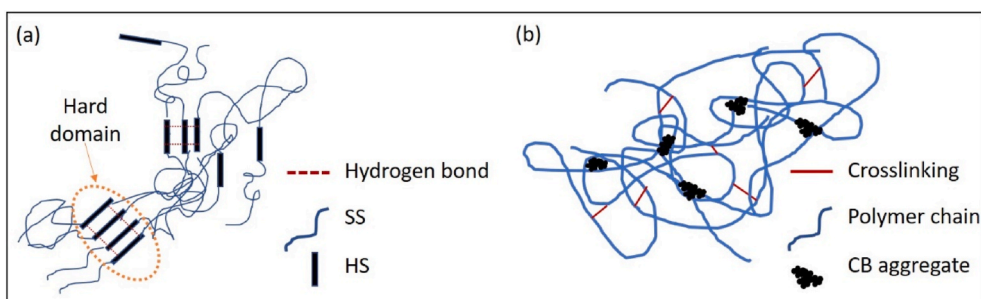The TPU is a polyester-polyurethane block copolymer kindly

Fig. 1. Example of network organization for TPUs (the hard domains act as physical crosslinks) (a) and filled and chemically crosslinked rubbers (b).

provided by BASF (commercial name: EC 60 A 10 P Elastollan©). The volume fraction of hard segments $\varphi = 0.24$ and the average distance $L = 12–15$ nm between hard domains was estimated from X-Ray diffraction of pristine samples using the lamellar model Fourier analysis [19,20]. The glass transition temperature (T_g) of -50 °C was obtained by Differential Scanning Calorimetry (DSC) at $10°$/min. PS samples were injection moulded in a BOY 50 M injection moulding machine (Boy machines Inc., US) at the French Rubber and Plastics Research and Testing Laboratory (LRCCP) using the procedure recommended by BASF. The temperature used in the injection procedure is summarized in Table 1. We remark that in TPUs the injection procedure may induce a preferential orientation which in turn would affect the final result. In order to overcome this difficulty, in this study all PS samples were injected so that the largest side perpendicular to injection direction.

2.2. Large strain tensile tests

Uniaxial tensile tests were performed on dog-bone samples (with a cross section of 2×4 mm cut from a square plate) using an Instron 5590 tensile machine (capacity of 2 kN). The samples were deformed at constant stretch rate $\dot{\lambda} = 4 \ s^{-1}$ up to rupture or in cyclic conditions at the same $\dot{\lambda}$. In the second case, 10 cycles were performed up to maximum stretch of 20, 40 and 100% of the stretch at break λ_b.

2.3. Dynamic mechanical analysis (DMA)

DMA analysis was performed on circular disks of 10 mm diameter and 2 mm thickness cut from a square plate using a METRAVIB (DMA+450 series, FR). Two cylinders are glue to three metallic supports placed in metallic grips. The middle support moves and generates an oscillatory displacement up and down between 0.005% and 100% of strain at temperature of 23 °C and frequency of 10 Hz.

2.4. Fracture toughness

Fracture toughness and cyclic fatigue tests were carried out using PS samples of length $= 45$ mm, height (h_0) $= 5$ mm and thickness $= 1$ mm with a single crack of 22 mm cut along the direction parallel to the sample's length. Each cut was made in non-relaxing conditions on the clamped sample and after the application of a small pre-stretch. For measuring the fracture toughness Γ, the material was stretched stretch rate $\dot{\lambda} = 4 \ s^{-1}$ up to fracture. The minimum stretch to propagate the crack λ_c is determined from the point where the stress undergoes a maximum value in the stress-stretch curve of notched samples using the same procedure adopted in other works [21,22]. At the crack propagation conditions the equivalence $G = \Gamma$ holds [16] and the value of fracture toughness is defined as $\Gamma = W(\lambda_c)h_0$ where $W(\lambda_c)$ is calculated by integrating the stress-stretch loading curve of pristine PS samples between λ and λ_c .

2.5. Cyclic fatigue in styrene-butadiene rubber

We used SBR rubber filled with carbon black. The SBR has a mass M_n of 120 kg/mol and a polydispersity of 1.94 and was provided by the Michelin research centre. Its styrene content is 15 wt% and T_g measured by differential scanning calorimetry (DSC at 10 °C/min) is -48 °C (very similar to that obtained for unfilled TPU). The detailed composition is reported in Table 2 as provided by Michelin:

Table 1
Barrel temperature profile for the injection procedure. Zones 1 to 4 are located between the rear and the front of the barrel.

Barrel	Zone 1 (°C)	Zone 2 (°C)	Zone 4 (°C)	Nozzle (°C)	Mold (°C)
TPU	165	170	175	170	30

Table 2
SBR composition in PHR. Filler content and crosslinking density are reported in volumetric fraction (data from ([24]). Note that N347 is a type of carbon black, Sulfur is a crosslinking agent, Struktol™ and N-Cyclo-hexyl-2-benzothiazole sulfenamide (CBS) are accelerators to vulcanize the rubber, and N-(1, 3-dimethylbutyl)-N′-phenyl-*p*-phenylenedi-amine (6PPD) is an anti-oxidant.

SBR	100
N347	5
6PPD	1
Struktol	3
CBS	1.5
Sulfur	1.5
φ	0.03
ν	$8.1 \cdot 10^{-5}$

All samples were prepared, moulded and cured by Michelin. For tensile tests, samples were cut in a dog-bone shape with a cross section of 2×4 mm and loaded at a stretch rate $\dot{\lambda} = 4 \ s^{-1}$. For crack propagation experiments, pure shear samples were moulded in two geometries. PS_{large}: length $= 157$ mm, height $= 13$ mm, thickness $= 2$ mm and PS_{small}: length $= 35$ mm, height $= 6$ mm, thickness $= 0.8$ mm. Uncracked samples were preconditioned at $\lambda_{max} = 1.27$ for 1000 cycles to get rid of transient effects and used to calculate $G(\lambda) = W(\lambda)h_0$. For each preconditioned sample two edge cracks and a centre crack were cut with a fresh razor blade in the direction parallel to the sample's length. Then the notched samples were strained for 50.000 cycles at values of G corresponding to $\lambda < \lambda_{max}$ to accommodate the crack tip before starting the measurement of dc/dn. All tests were performed at 10 Hz.

3. Materials characterization

3.1. Small strain properties

The filled SBR and TPU have similar values of the storage shear modulus μ' at low strain, and both materials display a decreasing modulus with applied strain accompanied by an increase of Tan δ, as shown in Fig. 2. This strain softening, known as Payne effect, is common in filled rubbers and is generally associated to the onset of damage of the filler network [23]. The comparative analysis allows to appreciate that SBR and TPU present a similar form of damage, but it occurs at larger strains in TPU ($\sim 10\%$). Moreover, the small strain regime in TPU is less dissipative (lower Tan δ). Both these observations reflect a more elastic character with limited structure modifications up to 10% strain in TPU.

3.2. Uniaxial tensile tests

Fig. 3 (a) shows representative stress-strain curves for TPU and filled SBR. The linear regime is only observed for $\lambda < 1.2$ and is similar for both materials as underlined by the close values of small strain moduli estimated by calculating the linear fitting of the stress-stretch curve between $\lambda = 1$ and *1.15*. The values of the modulus are reported in Table 3 (data from Ref. [24]) along with the values of strength σ_b and stretch λ_b at break for both materials.

After the linear regime, both materials display stress-softening followed by strain-hardening although to a very different extent. Among all factors contributing to the mechanisms of crack growth, viscoelastic dissipation is known to play an important role in elastomers [25,26]. In Fig. 3 (b) we show uniaxial step-strain cycles of deformation for TPU and SBR. Both materials exhibit cyclic hysteresis that is more pronounced in the first cycle and then gradually decreases in the following ones. This phenomenon also known as Mullins effect, was already observed both in filled rubbers and unfilled TPU [27,28]. Although there is no generally accepted microscopic explanation, the Mullins effect is often attributed
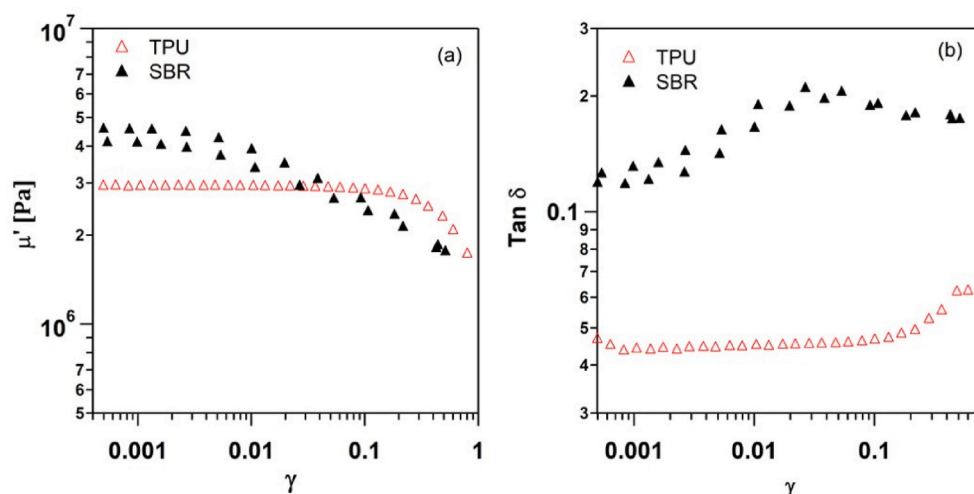
Fig. 2. Storage modulus (a) and Tan δ (b) vs. dynamic strain amplitude for TPU and SBR at 23 °C and 10 Hz.
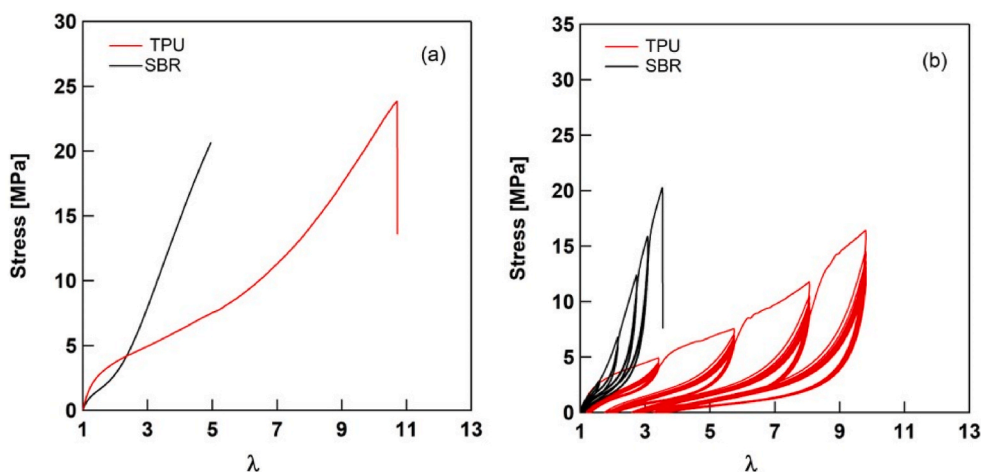

Fig. 3. Uniaxial nominal tensile test at 23 °C for TPU (red) and SBR (black) up to failure (a) and in cyclic experiments (b). (For interpretation of the references to colour in this figure legend, the reader is referred to the Web version of this article.)

Table 3
Linear modulus, stretch and stress at break and toughness of TPU and SBR (data from Ref. [24]).

	E [MPa]	λ_b	σ_b [MPa]	Γ [kJ/m²]
TPU	7.3	10.8	24.7	138
	±0.12	±1.9	±2.3	±13
SBR	8.2	3.6	16.6	23
	± 0.5	± 0.1	± 1.1	± 3

to structural modifications of the filler network or of the hard domains respectively for filled rubbers and unfilled TPUs [27,29,30]. It is important to note that despite its thermoplastic character, the fraction of dissipated energy at fixed applied strain is lower for TPU than for filled SBR. This is true in the 1st cycle, characterizing damage (Fig. 4(a)) and in the 10th cycle (Fig. 4(b)) representing stabilized cycling conditions where an excessive hysteretic behaviour is often undesirable, since it may lead to heat build-up, reducing the material's ability to resist crack propagation.

3.3. Fracture toughness

Table 3 also reports the value of Γ calculated for notched SBR and TPU. Despite similar linear properties of the two materials, TPU is almost one order magnitude tougher than the SBR filled rubber at 23 °C indicating clearly that large strain properties (that predominate around the crack tip singularity) play an important role in the toughness.

4. Results and discussion

4.1. Effect of the loading conditions

The fatigue resistance of TPU samples was probed with two different loading protocols as schematically shown in Fig. 5: either a minimum value of stress $\sigma_{min} = 0$ was imposed at each cycle (Protocol A) or the sample was unloaded to the displacement corresponding to its initial length ($\lambda_{min} = 1$) (Protocol B), as it is classically done for SBR.

With Protocol A, the sample is strained between an imposed λ_{max} and a variable minimum stretch λ_{min}, corresponding to the imposed condition $\sigma_{min} = 0$, that increases in time due to residual plastic strain experienced by the sample, as illustrated in Fig. 5 (a). Therefore, the applied value of G decreases with the number of cycles until a steady-state (or shake down) is reached [31,32].

With Protocol B the sample is strained between imposed nominal values of both λ_{max} and $\lambda_{min} = 1$, implying that the sample will undergo compressive stresses and buckle when the stretch decreases below the residual plastic stretch λ_{res}, as illustrated in Fig. 5(b).

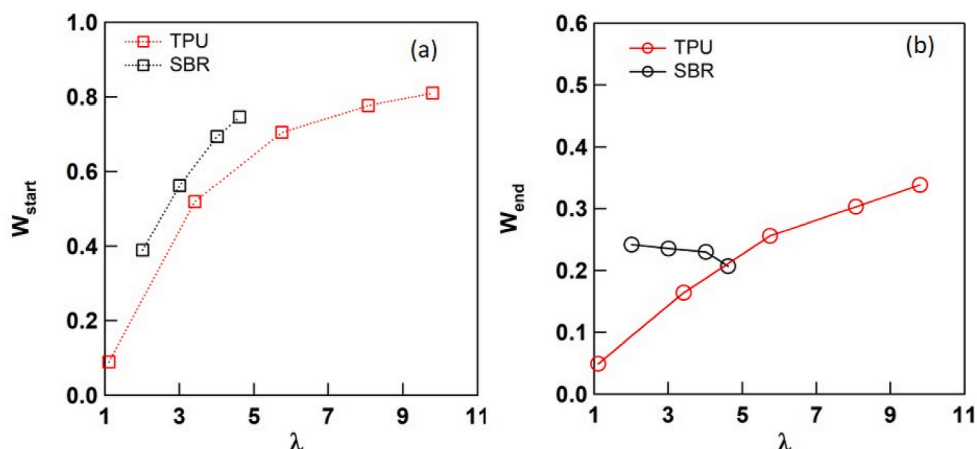In classical rubbers the two loading schemes A and B are

Fig. 4. Ratio between the dissipated and the provided energy in the first (a) and the 10th (b) cycle of the uniaxial cyclic experiments.
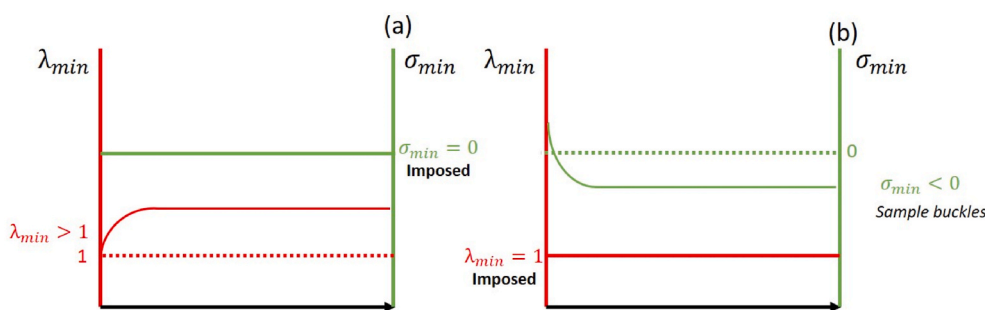

Fig. 5. Schematic of minimum stretch λ_{min} and minimum stress σ_{min} as function of the number of cycles during a fatigue experiment for Case A (a) and B (b).

substantially identical, since the residual plastic strain is generally negligible and it stabilizes after a few cycles.

4.2. Evaluation of G in TPU

As discussed in the introduction, we did not use any pre-conditioning procedure in TPU, unlike what is classically done for filled chemically crosslinked rubbers. Fig. 6 (a) shows the stress-stretch curve for TPU at λ = 2.2 for the 1st, 200th, 5.000th and 10.000th cycle and the corresponding values of G as a function of the number of cycles are reported in Fig. 6 (b). Most of the softening and the accumulation of plastic strain

occurs over the first cycles of the experiment, the stress-stretch curve eventually stabilizes between 5.000 and 10.000 cycles and the value of G is very stable during further cycles. Even after this shake-down, the stress-stretch curve of TPU shows a residual hysteresis, as it is also the case for classical thermoset rubbers. Nevertheless, as previously indicated for uniaxial cyclic experiments, for the same value of maximum stretch the hysteresis is comparable or lower for TPU. Fig. 7 shows an example of stabilized curve of TPU obtained with the protocols A (a) and B (b). The value of elastic energy density per cycle ($W(\lambda)$) was always calculated using the positive area below the unloading curve (shaded in Fig. 7 (a) and (b)). Interestingly, for comparable values of the maximum
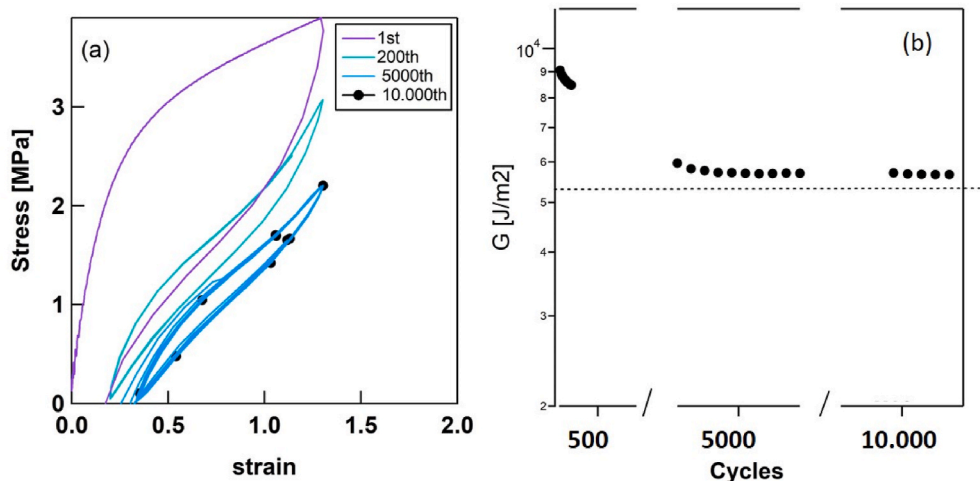

Fig. 6. Stress-stretch curve of TPU strained at λ = 2.3 (a) and corresponding G as function of the number of cycles (b).
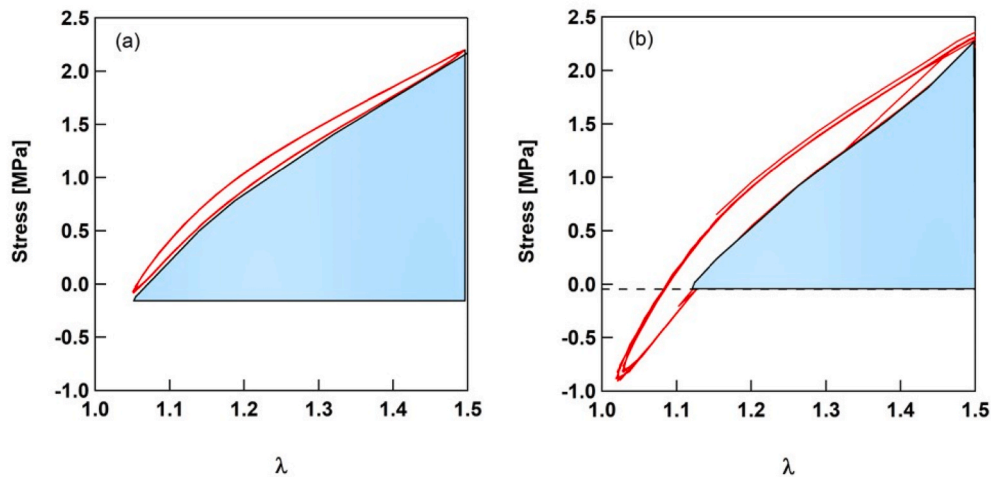
Fig. 7. Stress-stretch curve for the stabilized cycle obtained using method A (a) and B (b). The shaded area represents the stored elastic energy density used in the calculation of G.

stretch, the unloading path of the stress-stretch curve is not much affected by the protocol (A or B) and the calculated values of $W(\lambda)$ (and thus G) overlap (as it can be appreciated in Fig. 8) while, on the other side, in case B the stress-stretch curve per cycle results in a higher hysteresis than method A. Fig. 8 reports the values of $G(\lambda)$ obtained without any pre-conditioning but using the 10.000th unloading curve (after shake-down) for different values of increasing applied deformation for both protocols A and B. All the data can be consistently fitted with a linear relationship for the curve $G(\lambda)$.

4.3. Fatigue failure

Once $G(\lambda)$ has been experimentally calibrated on unnotched samples, crack propagation experiments under cyclic loading were carried out on notched samples for a different number of cycles at different values of applied stretch corresponding to the selected values of $G(\lambda)$. For each fatigue experiment, we evaluated the crack length c during the cycles by taking images of the crack tip at regular time intervals and identifying

Fig. 8. Example of calculated G vs. λ for TPU without pre-conditioning. G is calculated using the stress-stretch curve of the 10.000th cycles for each value of the increasing applied stretch. The data for method A and B overlap.

the maximum value of the x-coordinate of the contour of the crack in the open position, as shown in Fig. 9(a). The crack profile is clearly blunted rather than sharp in TPU. To quantify the difference in crack shape between TPU and SBR in a classical cyclic fatigue experiment, we calculated the crack tip radius in the open position using a parabolic fitting (yellow line in Fig. 9(a). Fig. 9(b) reports an example of the fitted radius for TPU (Protocol A) and SBR tested at: G~ 10.000 J/m^2 and G~ 1.800 J/m^2 respectively, corresponding to similar values of dc/dn for both materials. After a first transient stage, where the crack tip changes shape, both TPU and SBR show a constant value of the fitted radius. In similar propagation conditions, TPU shows a considerably blunted profile and a higher radius than SBR according the higher value of G (and λ) required to the propagate the crack in cyclic fatigue.

Fig. 10 (a,b) reports the crack length c as a function of the number of cycles for TPU tested either with protocol A (no buckling) or with protocol B. In the case of protocol A, at the beginning of the experiment, the crack extension per cycle is higher and gradually approaches a steady state growth rate (constant dc/dn). This behaviour, may be related to stress accommodation: in the first cycles in fact, the stress singularity around the crack tip is more pronounced and the material is not "accommodated" yet. Moreover, in the case of TPU the residual plastic strain in the bulk is not stabilized yet. To evaluate the value of crack propagation per cycle expressed as dc/dn we only considered the data points after 10.000 cycles and we evaluated the slope of the curve c vs. the number of cycles.

In the case of protocol B, the crack increases almost linearly with the number of cycles, and we also evaluated the slope of the curves above 10.000 cycles as is conventional. The final results of cyclic crack propagation for TPU tested with both protocols and for SBR, are reported in Fig. 10 (c) as dc/dn vs. applied G. In case of SBR, the values of dc/dn obtained for PS$_{small}$ (which has dimensions comparable with those used in TPU) were took from the PhD thesis of Mzabi [33] who showed the perfect overlapping with those evaluated using PS$_{large}$ [24]. This result confirms the independency of G on the sample dimensions in SBR and allows a robust comparison with the data obtained in TPUs that are exclusively for small PS. In case of TPU, the values of dc/dn in the whole range of tested G are always higher for the protocol B than protocol A. This is probably a consequence of the systematic buckling of the specimen during unloading cycles in protocol B which is likely to damage the sample along the main fold in the centre, leading to lower fatigue resistance. It is also interesting to discuss the "threshold" value G_t required to propagate the crack in TPU and SBR. According to Lake and Lindley [17,34], in vulcanized rubbers G_t can be estimated using the extrapolation of the linear part of the curve dc/dn vs. G. In absence of
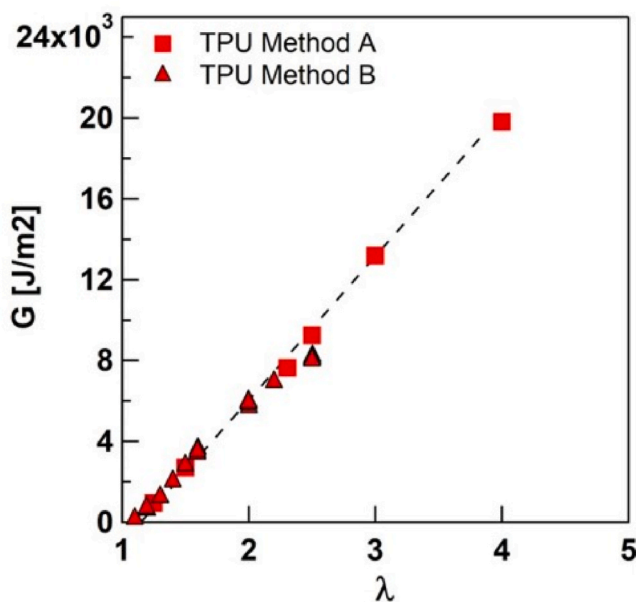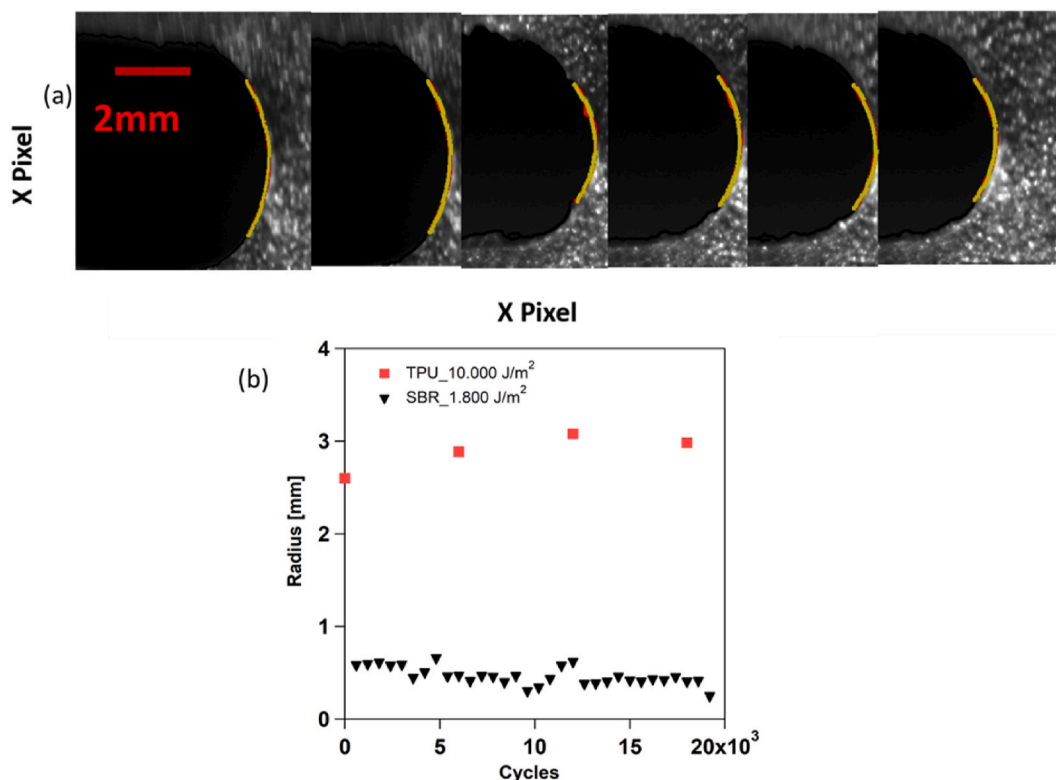
Fig. 9. Example of crack profile and parabolic fitting during cycles (a) and calculated radius for TPU and SBR in a cyclic fatigue experiment at similar crack propagation rate, dc/dn (b).

this linear regime in TPU, we decided to provide a higher bound for G_t based on the resolution of the optical system for both protocols A and B. In both cases we run at least 36.000 cycles and the resolution of the optical system was ~ 38 μm. Under this condition the minimum detectable crack growth was ~ 1 nm. Using this definition, dc/dn < 1 nm/cy at $G_t < 2600$ J/m^2 for protocol A and $G_t < 1000$ J/m^2 for protocol B. Both these values are surprisingly high compared to classical thermoset rubbers, which generally show typical values of G_t between 40 and 70 J/m^2 [17,36,41].

A remark must be done concerning the effect of preconditioning step on crack propagation. Contrary to TPU, SBR samples were cyclically strained at deformation larger than those used in cyclic fatigue at the beginning of each test. This step is likely to induce some damage in the material and to negatively affect the final value of propagation resistance. Nevertheless, the difference in terms of both G_t and dc/dn vs. G between TPU (especially in protocol A) and SBR is so marked that the effect of any possible damage induced by the preconditioning in SBR can be considered negligible confirming the conclusion that TPU are highly fatigue resistant material.

5. Discussion

The results of this paper highlight two important elements in the cyclic crack propagation behaviour of TPU compared to crosslinked rubbers: a) TPUs have higher G_t than those of common elastomers, b) the linear regime in dc/dn vs. G typically found in crosslinked rubbers, is replaced by a fast transition between not propagating crack and fast propagating crack (or power law regime). We also showed that the fatigue resistance of TPU is affected by the specific testing procedure, and in case of buckling of the sample during cycles (caused in principle by the residual deformation) dc/dn is significantly increased by mechanical damage on the folding line.

The methodology presented to evaluate G is compatible with large deformations of soft materials as far as the dissipative process zone at the

crack tip remains smaller than the sample's dimensions. As discussed in Ref. [37], the size of the process zone can be estimated from the radius of the loaded crack tip, which should remain small in front of the height of the PS sample. This condition is fulfilled in the whole regime of fatigue propagation in SBR, and also in the neighbourhood of the threshold of fatigue propagation in TPU. On the other hand, in the most sever conditions and for the highest value of G applied to TPU in present analysis (Fig. 9), the blunting radius becomes comparable with the sample height. For this very large strain regime, the independence of the crack propagation curves dc/dn vs. G from sample dimension should thus be carefully checked in the future using larger samples. This was not possible in the present analysis, since it is very difficult to obtain a large, thin and homogeneous PS sample by injection, due the very high viscosity of melted TPU.

6. Conclusion

We have proposed an approach to evaluate cyclic fatigue resistance in TPUs using the framework of fracture mechanics as developed for cross-linked elastomers. We showed that compared to methods used for classical filled elastomers, a different protocol is required to account for time-dependent properties and permanent strain of TPUs. This must include a control in force of the minimum of each cycle to avoid the phenomenon of buckling which can in turn damage the material inducing higher dc/dn. Moreover, we demonstrated that TPUs possess typical values of fracture toughness and a cyclic fatigue threshold (where dc/dn < 1 nm/cy) almost one order of magnitude larger than those of filled SBR rubbers with similar values of small strain modulus. This implies that TPUs may either resist for more cycles than classical rubbers when similar energy release rates are applied, or may sustain larger strains with only moderate crack growth when rubbers would fail in a single cycle. This result confirms that TPUs possess the combination of high fatigue threshold and low stiffness that is strongly desirable for practical applications and still missing in conventional elastomers as
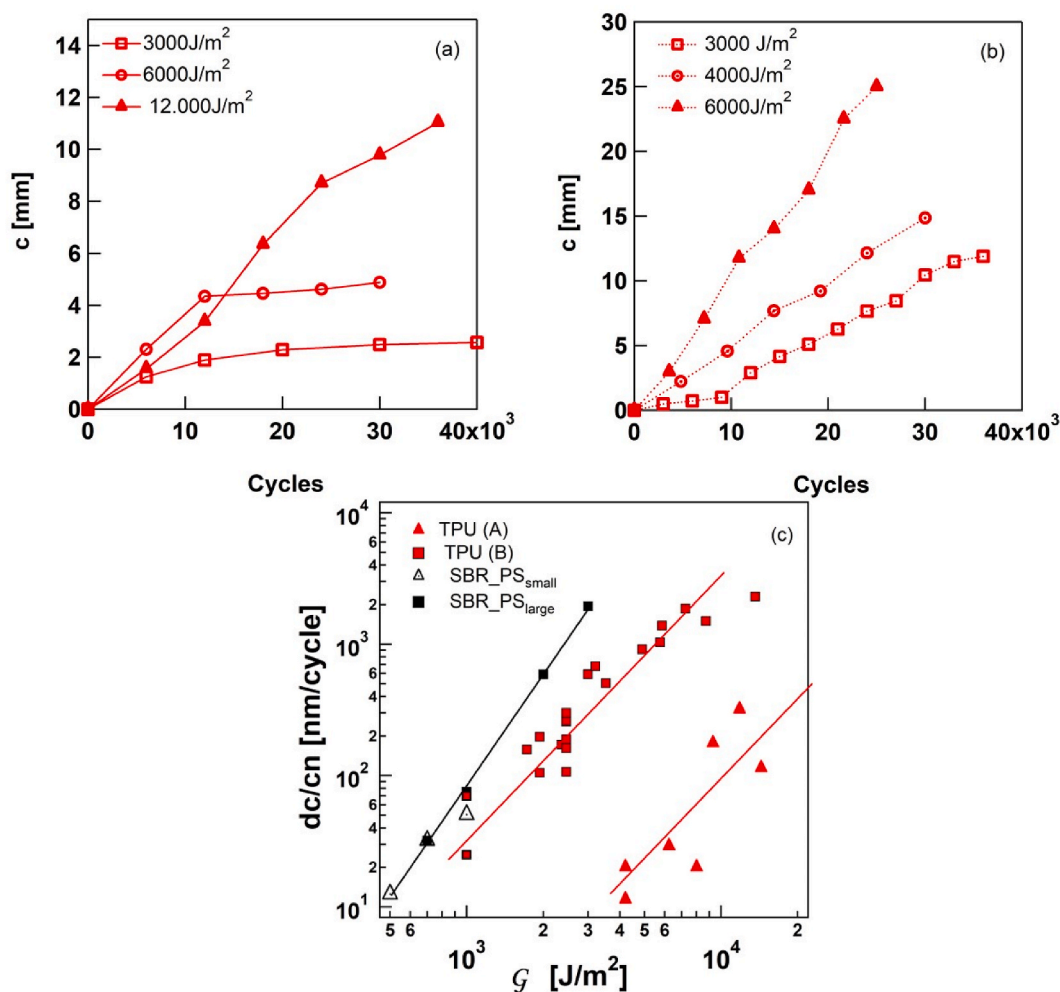
Fig. 10. Crack length vs. cycles for TPU tested with protocol A (a) and protocol B (b) for different values of the applied G(λ). Crack propagation per cycle (dc/dn) vs. G for TPU (protocol A and B) and SBR (c).

proved by the numerous attempts to develop high fatigue resistance elastomers implementing different complex techniques [38–40].

Author contributions

Research was designed by G.S., N.S., P.H., M.C., C.C. Specimens were mechanically tested by G.S. The manuscript was written by G.S. and critically revised by all authors. All authors have given final approval to the final version of the manuscript. All data needed to evaluate the conclusions in the paper are present in the paper and/or the Supplementary Materials. Additional data available from authors upon request.

Declaration of competing interest

The authors declare that they have no known competing financial interests or personal relationships that could have appeared to influence the work reported in this paper.

References

[1] G. Holden, Thermoplastic elastomers, Appl. Plast. Eng. Handb. (Jan. 2011) 77–91.
[2] Y.L. Tee, M.S. Loo, A. Andriyana, Recent advances on fatigue of rubber after the literature survey by Mars and Fatemi in 2002 and 2004, Int. J. Fatig. 110 (2018) 115–129.
[3] W.V. Mars, A. Fatemi, A literature survey on fatigue analysis approaches for rubber, Int. J. Fatig. 24 (9) (2002) 949–961.
[4] Z. Major, M.C. Miron, U.D. Cakmak, Characterization of thermoplastic elastomers for design efforts, Adv. Mater. Res. 905 (2014) 161–166.
[5] Z. Major, M. Isasi, T. Schwarz, Characterization of the fracture and fatigue behavior of thermoplastic elastomer materials, Key Eng. Mater. 417 (418) (2010) 789–792.
[6] W.V. Mars, M.D. Ellul, Fatigue characterization of a thermoplastic elastomer, Rubber Chem. Technol. 90 (2) (2017) 367–380.
[7] R. Bonart, X-ray investigations concerning the physical structure of cross-linking in segmented urethane elastomers, J. Macromol. Sci. Part B 2 (1) (1968) 115–138.
[8] B.S. Hsiao, S. Kohjiya, M. Tosaka, A.H. Tsou, S. Datta, Synchrotron X-ray studies of vulcanized rubbers and thermoplastic elastomers, Rubber Chem. Technol. 79 (3) (2006) 460–488.
[9] J.W.C. Van Bogart, A. Lilaonitkul, S.L. Cooper, Morphology and Properties of Segmented copolymers 176, American Chemical Society, 1979, pp. 3–30.

[10] F. Yeh, B.S. Hsiao, B.B. Sauer, S. Michel, H.W. Siesler, In-situ studies of structure development during deformation of a segmented poly(urethane-urea) elastomer, Macromolecules 36 (6) (1954) 1940, 2003.

[11] W.V. Mars, A. Fatemi, Factors that affect the fatigue life of rubber: A literature survey, Rubber Chemistry and Technology 77 (3) (2004) 391–412.

[12] S.M. Cadwell, R.A. Merrill, C.M. Sloman, F.L. Yost, Dynamic fatigue life of rubber, Ind. Eng. Chem. - Anal. Ed. vol. 12 (1) (1940) 19–23.

[13] Y. Marco, I. Masquelier, V. Le Saux, P. Charrier, Fast prediction of the wöhler curve from thermal measurements for a wide range of NR and SBR compounds, Rubber Chem. Technol. 90 (3) (2017) 487–507.

[14] A.G. Thomas, Rupture of rubber V cut growth in natural rubber vulcanizates, Rubber Chem. Technol. 32 (2) (1958) 477–489.

[15] G.J. Lake, Fatigue and fracture of elastomers, Rubber Chem. Technol. 68 (3) (1995) 435–460.

[16] R.S. Rivlin, A.G. Thomas, Rupture of rubber. I. Characteristic energy for tearing, J. Polym. Sci. 10 (3) (1953) 291–318.

[17] G.J. Lake, P.B. Lindley, Mechanical fatigue limit for rubber, J. Appl. Polym. Sci. 9 (1965) 1233–1251.

[18] O.H. Yeoh, Fracture mechanics of bond failure in the 'pure shear' test piece, Rubber Chem. Technol. 76 (2) (2003) 483–494.

[19] G.R. Strobl, M. Schneider, Direct evaluation of the electron density correlation function of partially crystalline polymers, J. Polym. Sci. 2 Polym. Phys. 18 (6) (1980) 1343–1359.

[20] J.T. Koberstein, T.P. Russell, Simultaneous SAXS-DSC study of multiple endothermic behavior in polyether-based polyurethane block copolymers, Macromolecules 19 (3) (1986) 714–720.

[21] E. Zhang, R. Bai, X.P. Morelle, Z. Suo, Fatigue fracture of nearly elastic hydrogels, Soft Matter 14 (18) (2018) 3563–3571.

[22] J.Y. Sun, X. Zhao, W.R.K. Illeperuma, O. Chaudhuri, K.H. Oh, D.J. Mooney, J. J. Vlassak, Z. Suo, Highly stretchable and tough hydrogels, Nature 489 (7414) (2012) 133–136.

[23] A.R. Payne, Hysteresis in rubber vulcanizates, J. Polym. Sci., Polym. Symp. 48 (1) (1974) 169–196.

[24] S. Mzabi, D. Berghezan, S. Roux, F. Hild, C. Creton, A critical local energy release rate criterion for fatigue fracture of elastomers, J. Polym. Sci., Part B: Polym. Phys. 49 (21) (2011) 1518–1524.

[25] B.N.J.J. Persson, O. Albohr, G. Heinrich, H. Ueba, Crack propagation in rubber-like materials, J. Phys. Condens. Matter 17 (44) (2005).

[26] Y. Morishita, K. Tsunoda, K. Urayama, Velocity transition in the crack growth dynamics of filled elastomers: contributions of nonlinear viscoelasticity, Phys. Rev. E 93 (4) (2016) 1–11.

[27] T. Sui, S. Ying, G. Sun, et al., Strain softening of nano-scale fuzzy interfaces causes Mullins effect in thermoplastic polyurethane, Sci. Rep. 7 (1) (2017) 1–9.

[28] H.J. Qi, M.C. Boyce, Stress-strain behavior of thermoplastic polyurethanes, Mech. Mater. 37 (8) (2005) 817–839.

[29] L. Mullins, Softening of rubber by displacement, Rubber chemistry and technology 42 (1) (1969) 339–362.

[30] J. Diani, B. Fayolle, P. Gilormini, A review on the Mullins effect, Eur. Polym. J. 45 (3) (2009) 601–612.

[31] W. Zhang, X. Liu, J. Wang, et al., Fatigue of double-network hydrogels, Eng. Fract. Mech. 187 (2018) 74–93.

[32] R. Bai, Q. Yang, J. Tang, X.P. Morelle, J. Vlassak, Z. Suo, Fatigue fracture of tough hydrogels, Extrem. Mech. Lett. 15 (2017) 91–96.

[33] S. Mzabi, PhD thesis. Caractérisation et analyse des mécanismes de fracture en fatigue des élastomères chargés, Sorbonne Université, Paris, 2010, pp. 1–310.

[34] P.B. Lake, G.J. Lindely, Cut growth and fatigue of rubbers. II.Experiments on a noncrystallizing rubber, J. Appl. Polym. Sci. 8 (2) (1964) 707–721, https://doi.org/10.1002/app.1964.070080212.

[36] A.K. Bhowmick, Threshold fracture of elastomers, J. Macromol. Sci. Part C 28 (3–4) (1988) 339–370.

[37] C. Creton, M. Ciccotti, Fracture and adhesion of soft materials: a review, Rep. Prog. Phys. 79 (4) (2016) 46601.

[38] C. Li, H. Yang, Z. Suo, J. Tang, Fatigue-Resistant elastomers, J. Mech. Phys. Solid. 134 (2020) 1–12.

[39] C. Xiang, Z. Wang, C. Yang, X. Yao, Y. Wang, Z. Suo, Stretchable and fatigue-resistant materials, Mater. Today 34 (2020) 7–16.

[40] Z. Wang, C. Xiang, X. Yao, P. Le, J. Mendez, Z. Suo, Stretchable materials of high toughness and low hysteresis, Proc. Natl. Acad. Sci. U.S.A. 116 (13) (2019) 5967–5972.

[41] P.B. Lake, G.J. Lindely, Fatigue of rubber at low strains, J. Appl. Polym. Sci. 10 (2) (1966) 343–351. https://doi.org/10.1002/app.1966.070100214.